AIAA SciTech Forum
11–15 & 19–21 January 2021, VIRTUAL EVENT
AIAA Scitech 2021 Forum

10.2514/6.2021-0422

Preliminary Design of a Distributed Telescope CubeSat Formation for Coronal Observations

Athreya R. Gundamraj[1], Rohan Thatavarthi[1], Christopher A. Carter[1], E. Glenn Lightsey[2]
Georgia Institute of Technology, Atlanta, GA 30332, United States

Adam W. Koenig[3], Simone D'Amico[4]
Stanford University, Stanford, CA 94305, United States

This paper presents the preliminary system design of the Virtual Super-resolution Optics with Reconfigurable Swarms (VISORS) mission, a multi-CubeSat distributed telescope which will image the solar corona to investigate the existence of underlying energy release mechanisms. VISORS was conceived in the National Science Foundation (NSF) CubeSat Innovations Ideas Lab Workshop held in 2019 to address NSF science goals with innovative technologies. This mission will gather imagery that directly pertains to theories of coronal heating. In the paper, novel technologies are described that enable the VISORS mission to meet its challenging requirements and achieve the mission and science goals. The VISORS formation is composed of two 6U CubeSats that fly 40 meters apart during science imaging as a distributed space telescope, with the lead spacecraft containing the optics and the trailing spacecraft containing the detector. An orbit maneuver planner utilizes GNSS carrier-phase measurements to provide a high-precision navigation solution, and a series of ceramic antenna arrays employ a novel 5.8 GHz inter-satellite crosslink. A 3 degrees-of-freedom (3DOF) propulsion system provides the capability for formation adjustments and active collision avoidance. The remaining spacecraft functions are handled by a spacecraft bus supplied by a commercial vendor, and the system integration is conducted by the VISORS mission team. Careful analysis of the system design and concept of operations led to the development of a safety plan which significantly reduces the risk of collision in a large subset of off-nominal scenarios. With a completed preliminary design review in Q4 2020 and a projected launch date in late 2023, this collaboration among 10 different universities, NASA, and a commercial partner is an upcoming mission that will demonstrate a new assembly of highly equipped CubeSats and their ability to conduct a state-of-the-art science mission in a cost and time effective manner.

[1] Graduate Student, Georgia Tech Space Systems Design Lab, AIAA Student Member.
[2] Director, Georgia Tech Space Systems Design Lab, AIAA Fellow.
[3] Postdoctoral Scholar, Stanford Aeronautics & Astronautics Dept., AIAA Member.
[4] Assistant Professor, Stanford Aeronautics & Astronautics Dept., AIAA Associate Fellow.

I. Mission Introduction

A. Science Overview

The solar corona exhibits highly dynamic behavior which results in its temperature rising to 1000 times hotter than the visible surface of the Sun, and this extreme temperature difference remains an open problem in space plasma physics [1]. The primary hypothesis is that the coronal heating is confined to narrow, filamentary bands on the order of 100 kilometers in diameter. This conjectured existence of thin heat-release sites is significant as it pertains to an encompassing "major outstanding science question" in the National Science Foundation (NSF) Geospace Section planning document: "How magnetic reconnection works and operates in the solar atmosphere, within the solar wind, at the dayside magnetopause, and in the magnetotail to initiate and facilitate energy transfer between the different regions of the space environment" [2].

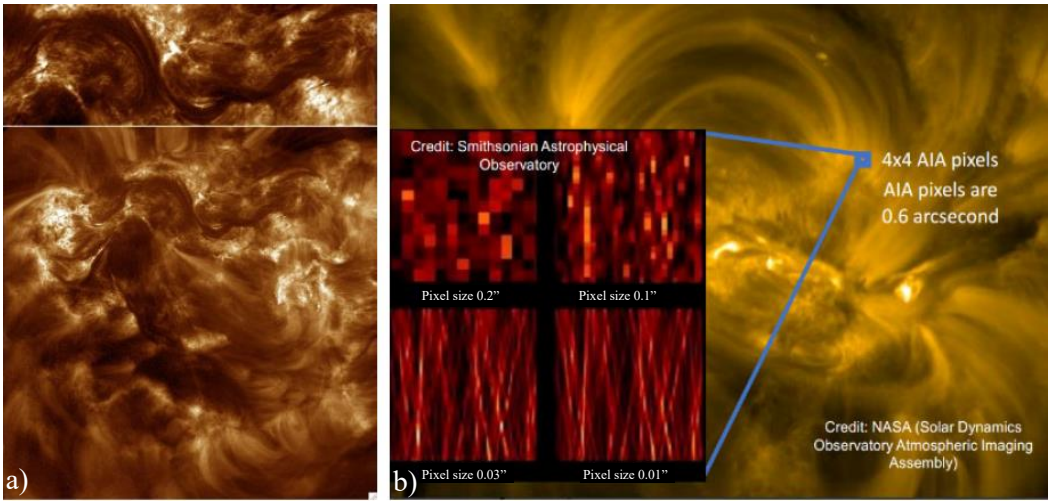

Fig. 1 a) Solar corona imagery using EUV optical systems b) simulated visual of heat-release sheets as an exploded view within an image of the corona.

Simulated imagery of the heat-release sheets, shown in comparison with existing extreme ultraviolet (EUV) imagery of the corona, are depicted in Fig. 1. The relative size of the coronal heating sheets is displayed in Fig. 1b and poses a challenging remote sensing problem: the imaging resolution required to observe the heat-release regions from Earth orbit is on the scale of 150 milli-arcseconds. Such performance is beyond the capabilities of existing EUV coronal imagers due to infeasible scaling requirements. Thus, a mission solution for this science problem, which was conceived at the NSF CubeSat Innovations Ideas Lab Workshop in 2019, employs a cube satellite (CubeSat) formation. This formation aligns to form a Sun-pointing "distributed telescope" in Low Earth Orbit and utilizes a diffractive-based imaging technology to collect coronal imagery at the required resolution. The mission is named "Virtual Super-resolution Optics using Reconfigurable Swarms" (VISORS), and it was selected by NSF in 2019 to proceed with a flight demonstration in 2023 or later.

B. Concept of Operations

The formation is comprised of two 6U CubeSats (30 cm x 20 cm x10 cm) that, when aligned, form a distributed telescope that captures images of the solar corona. The optics spacecraft (OSC) hosts the optics system of the telescope and serves as a sunshade to prevent unwanted solar radiation from entering the detector, which is hosted on the detector spacecraft (DSC). The DSC is located behind the OSC to form the Sun-OSC-DSC ordered alignment depicted in Fig. 2a. This alignment must be held for a minimum of 10 s for the detector system to capture usable coronal imagery. The alignment of the telescope is imperative to obtaining usable measurements of the corona, and great consideration has been placed to satisfying the stringent relative motion requirements discussed in Section II and depicted in Fig. 3.

The aforementioned Sun-OSC-DSC alignment occurs when the two spacecraft are in their science formation: a tighter formation in which the deputy spacecraft (the spacecraft responsible for relative maneuvering) performs ΔV maneuvers frequently to retain a separation of approximately 40 m which is the focal length of the telescope. When

preparing for the 10 s observation attempt, the deputy spacecraft completes a series of maneuvers such that at the time of observation, it drifts into the alignment displayed in Fig. 2a and Fig. 3. No thrust or slew maneuvers are conducted when in alignment as the motion would cause loss of focus with the telescope. Upon completion of the 10 s observation attempt, the deputy spacecraft reinitiates translational maneuvering to maintain its relative orbit. Due to the relative and absolute orbital mechanics, the formation can attempt a 10 s observation at the same orbital position each orbit. This availability is critical as it increases the probability of at least one observation attempt meeting the demanding relative state tolerances, which is the requirement for mission success. Preliminary Monte Carlo simulations of the formation demonstrate that the relative state requirements cannot be met for every observation attempt due to the expected distributions of measurement and process noise, so maximizing the number of attempts directly correlates to increasing the likelihood for mission success. This is under the assumption the common mode errors which occur in every observation attempt can be tuned out of the formation.

To perform autonomous maneuver planning and enable methods for active collision avoidance, the two spacecraft communicate their respective states with each other via an inter-satellite crosslink. When in the science formation, the crosslink is continually operational due to the high maneuver frequency and need for frequent GNSS measurement updates to minimize relative state uncertainties for observations. To obtain these GNSS measurements, each spacecraft shall be continually pointing its respective GNSS antenna toward a near-zenith direction when operating in science mode.

Upon completing a batch of observations, the formation autonomously executes maneuvers to transfer into a standby relative orbit with an inter-satellite separation of approximately 200 m. This standby orbit provides an inherent increase in spacecraft safety, saves propellant as maneuvers are performed less frequently for relative orbit maintenance, and reduces power usage as the larger relative separation allows for a reduced duty cycle for crosslink operation. Furthermore, each spacecraft will recharge their batteries, downlink image data and health metrics, and hold in this relative orbit until the next opportunity to gather coronal observations. When the operations team has completed data analysis from past observation attempts and selected a region of interest in the solar corona, the formation will receive an uplinked command with an updated inertial pointing vector to align with the telescope boresight with. The formation subsequently begins its transfer into the science formation and will attempt a new set of observations. This cycle between standby and science formations is repeated until the mission is complete, approximately 10 times over the mission lifetime. Fig. 2b depicts the concept of operations for the VISORS mission.

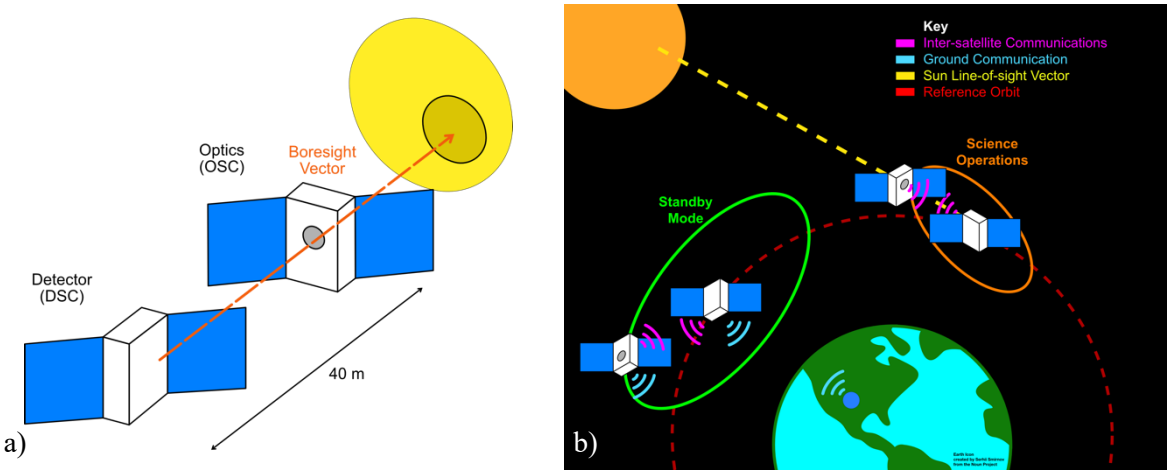

Fig. 2 a) Two 6U satellite formation when in alignment to collect coronal imagery b) VISORS concept of operations diagram.

The mission operations center for VISORS will be located at Georgia Tech with an additional ground station at Montana State University; both universities are partner institutions on the VISORS mission. The desired orbit is sun-synchronous and circular with an altitude between 500 km and 650 km. Sun-synchronous orbits provide a slow, predicable variation in the beta angle (defined as the angle between a sun-pointing inertial vector center on Earth and the projection of this vector onto the orbit plane). The altitude range balances a need for low aerodynamic drag and the ability to de-orbit within the standard 25-year requirement without expending propellant. The VISORS mission is

capable of being conducted in a larger subdomain of orbits which increases available launch opportunities, and these orbits are depicted in Table 1.

Table 1. Desired and acceptable range of orbit parameters for the VISORS mission.

Orbit Parameter	Desired	Range
Altitude (km)	600	500-650
Eccentricity	0.001	<0.01
Argument of Perigee (°)	Any	Any
Inclination (°)	98	30-150
Longitude of Ascending Node	10 AM/PM	8-11 or 1-4 AM/PM
Arg. of latitude for observation (°)	90	70-110 or 250-290

II. Key Requirements

A. High-Precision Relative Navigation

The telescope system distributed across the formation provides the required angular resolution to image the hypothesized sheet-like regions in the corona, but its sensitivity enforces strict requirements on the relative position and velocity errors when in alignment for data collection. The OSC deviation from the DSC in the lateral direction, the direction perpendicular to the boresight vector, is restricted to be within an 18 mm tolerance due to the boresight vector across the two vehicles that must be maintained, and due to the vignetting that occurs if unwanted EUV radiation enters the DSC. The OSC cannot shift in the longitudinal direction, the direction parallel to the boresight vector, past 15 mm with respect to the DSC to maintain the nominal focal length. Furthermore, not depicted in Fig. 3 is a requirement to hold the spacecraft lateral drift at a rate below 200 μm/s to prevent image blur. Longitudinal drift does not occur due to the relative orbit the spacecraft maintain when in science mode.

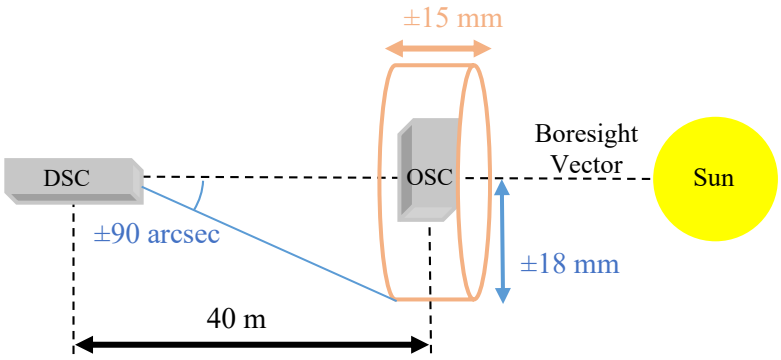

Fig. 3 Translational error tolerances for the VISORS formation when aligned for collecting observations.

B. Collision Avoidance

During operations, the miniscule distances between the satellites impose a risk of collision, especially when considering uncertainty propagation in off-nominal scenarios such as measurement blackout periods. A collision would be catastrophic, likely ending the mission while also creating a debris risk for other satellites in low Earth orbit. Thus, a key mission requirement is to have a formation relative orbit with passive collision safety. This is accomplished using E/I vector separation, as specified by D'Amico [4]. E/I vector separation describes an orbit where the relative eccentricity and inclination vectors are parallel or anti-parallel. This provides passive separation for a limited time, even in the presence of perturbations and uncertainty, by guaranteeing a minimum separation between

the spacecraft in the plane perpendicular to the flight direction. The passive safety degrades once the relative eccentricity and inclination vectors become perpendicular [4]. All maneuvers in standby orbit and a portion of maneuvers in science orbit serve as relative station keeping maneuvers to prevent such degradation and thus retain passive safety.

Beyond the passive collision safety provided by the E/I vector-separated relative orbit, it is necessary to ensure safety from collision in the event there of a failure on one or both spacecraft. A failure in this context refers to off-nominal spacecraft behavior that manifests in the inability to perform relative station keeping maneuvers for any duration of time. Under this situation, it may be necessary to use an active collision avoidance approach. Having an active collision avoidance plan imparts a requirement that each spacecraft must not only have accurate knowledge of the dynamic states of the formation but also the ability to compute and execute an escape maneuver in the event a future collision is detected. The specific mitigation plan for an active collision avoidance scenario is a function of the relative orbit, the failure mode exhibited on the spacecraft, and the time required for the inhibited spacecraft to return to nominal performance. Therefore, a holistic safety plan was developed by analyzing the spacecraft design with the concept of operations. This plan and its effectiveness in mitigating collision risk is discussed in a subsequent section.

C. Omnidirectional Communication

Accurate relative navigation and maneuver planning requirements flow to requirements for an inter-satellite communication crosslink. Using this inter-satellite link (ISL), the spacecraft transmit the required data, which includes GNSS pseudorange and carrier-phase measurements at different frequencies, for the guidance, navigation, and control (GNC) software to obtain the relative state accuracies depicted in Fig. 3. Furthermore, this communication crosslink also enables the capability for active collision avoidance by enabling both spacecraft to estimate the translational states of the entire formation. However, the pointing requirements which arise from the concept of operations entail that the spacecraft do not maintain a constant relative orientation throughout the mission. This consequence drives a requirement for omnidirectional communication: the capability to establish an ISL shall be independent of the attitude of each spacecraft. Omnidirectionality decouples the spacecraft attitude with establishing an ISL which is advantageous as it frees the spacecraft from an additional pointing constraint. This lifted constraint is critical in science mode as the spacecraft attitude must already adhere to a zenith-pointing requirement for the GNSS receiver and a simultaneous Sun-pointing requirement when collecting observations; a third pointing requirement for an ISL may not be feasible and would require careful component placement on each spacecraft. Furthermore, omnidirectionality also allows the formation to retain an ISL in the event of an attitude control error. This retainment is important in the safety plan as it enables the formation to continue with relative maneuver planning and execution after a subsystem-level failure.

D. 3 Degree-of-Freedom Propulsion

Both spacecraft require an onboard propulsion system which allows for relative maneuvers to be executed. The requirement for a 3 degree-of-freedom (3DOF) propulsion system arises from both the complexity of the concept of operations and the need for rapid translational maneuvers. Similar to the case for omnidirectional inter-satellite communication, adding a pointing requirement for the thruster nozzle prior to a burn may result in an over-constrained set of pointing vectors that the spacecraft cannot meet. Furthermore, limiting the nozzle directions requires additional time to be allotted for the spacecraft to slew and settle. The translational burns leading up to an observation attempt must be executed within less than a minute of one another to significantly increase the probability of a successful observation. Thus, slew maneuvers must be completed on the order of seconds which is not guaranteed considering that any two burn attitudes may have an eigenangle difference of up to 180^{o}. Rapidly slewing the spacecraft will likely violate the pointing requirements for the GNSS receiver and Sun-pointing direction and cause the star tracker to reacquire its attitude solution. Both consequences lessen the relative state accuracies experienced when in an observation attempt. Active collision avoidance is also improved with 3-axis propulsion as the spacecraft can perform separation burns without requiring a prerequisite slew that adds a lead time before translational maneuvers can be executed. Requiring a propulsion system to have nozzle directions such that 3DOF maneuverability is achieved reduces operational complexity by removing the need for slews while allowing the formation to meet its pointing and maneuver execution objectives when in science mode and preparing for an observation.

III. Preliminary Design

In order to meet the driving requirements of the mission, the VISORS team has proposed a novel, two 6U satellite configuration as shown in Fig. 4. The OSC is the satellite in closest proximity to the Sun and houses the photon sieve, which is a diffractive optic technique built upon the canonical Fresnel zone plate [1]. Unlike zone plates, the annular

sections of the photon sieve contain arc-shaped gaps that are excised to obtain increased optical flexibility. The cross section of the OSC on the sunline also acts as a sunshade to prevent unwanted EUV radiation from entering the detector. The DSC stores the camera, corresponding sensors, and a processor to capture the coronal imagery. The DSC maintains a different relative orientation with respect to the OSC in an observation attempt due to a requirement that the detector mirror must be close to the center of mass within a specified margin. This margin is only met with the DSC component placement shown in Fig. 4. The remainder of this paper focuses on the unique spacecraft subsystems that enable the mission to meet its science objectives and whose performance directly correlates with mission success.

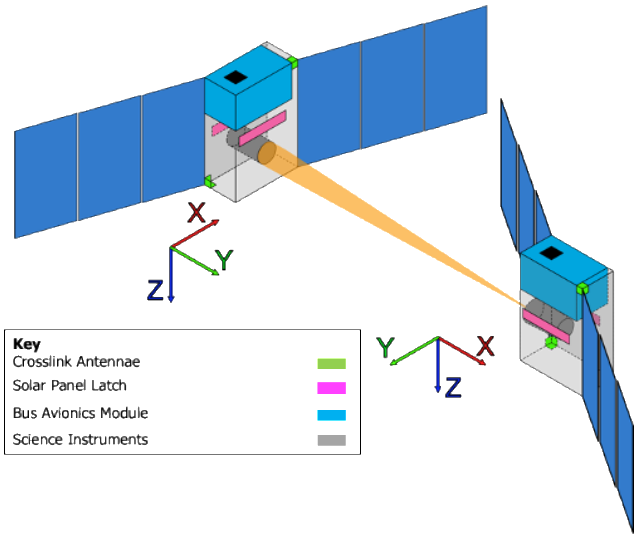

Fig. 4 Binary satellite configuration for VISORS mission. The OSC and DSC are on the top left and bottom right, respectively.

A. Spacecraft Bus

The spacecraft bus is responsible for the supplementary functions that each spacecraft must have to operate. The VISORS mission intends to use the Blue Canyon Technologies (BCT) 6U bus. One reason for this decision is the flight heritage and Technology Readiness Level-9 (TRL-9) of the BCT bus [5]. Furthermore, the spacecraft includes the BCT Avionics Module which contains several flight proven subsystems necessary for the mission: the XACT-15 Attitude Determination and Control System (ADCS), the Electrical Power System (EPS), the Command & Data Handling (C&DH), and the UHF Ground Communication system (COM). The XACT-15 also meets the precise attitude estimation and control requirements needed for science observation as proven by the ASTERIA mission [6]. The EPS includes a six solar panel array shown in the schematic Fig. 4 where 4 of the solar panels are fully populated. The EPS also includes batteries, necessary power delivery equipment, and power monitoring checks. Moreover, the bus includes the Novatel OEM719 GPS receiver that is compliant with the GNC software needed for relative orbit maneuvering as well. The ground communication system incorporates the SpaceQuest TRX-U UHF radio and a monopole antenna. In addition, the BCT flight computer allows allocation of computer resources to mission-specific software, reducing the need for additional processing elements in payload subsystems; the VISORS mission team intends to utilize this flexibility and host the GNC software on the BCT flight computer. Due to the flight proven nature of the BCT bus and its included components, the VISORS mission team can focus on the development of subsystems unique to this mission while avoided the increased risk of internally developing the subsystems that the BCT bus provides. The DSC spacecraft is shown in the Fig. 5 below, including the component placement of the key subsystems discussed in this paper. Fig. 6 shows the OSC spacecraft and its respective component placement.

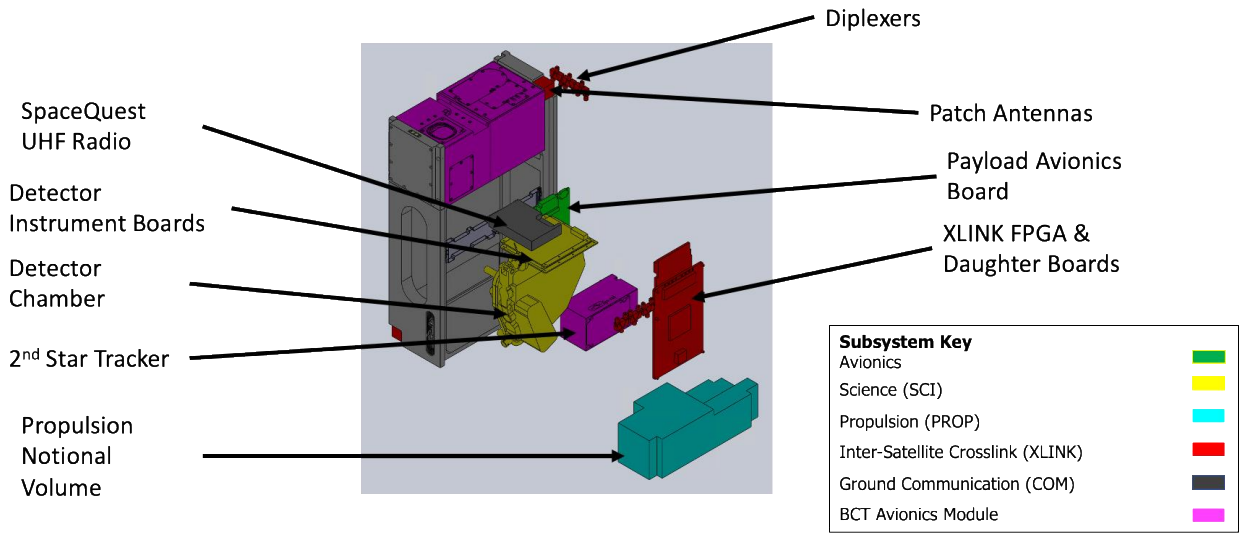

Fig. 5 DSC spacecraft and subsystem component placement. Solar panels are not shown.

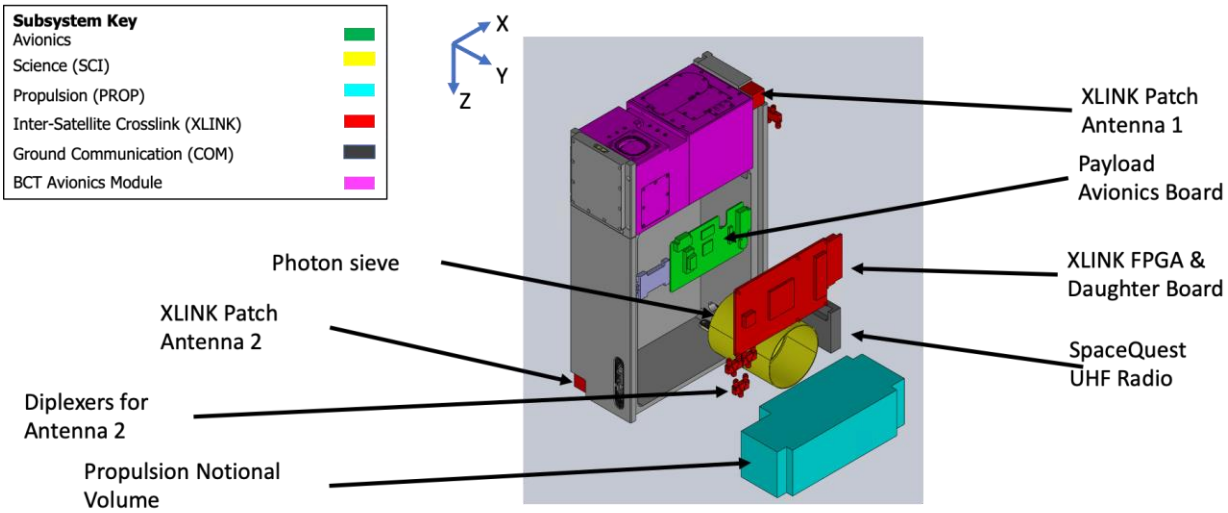

Fig. 6 OSC spacecraft and subsystem component placement. Solar panels are not shown.

B. Guidance, Navigation, and Control (GNC)

An accurate onboard navigation system is required to meet the relative motion control requirements during science observations. Stanford University, one of the partner institutions on the team, has a proposed a solution to the relative navigation challenges through their Distributed Timing and Localization (DiGiTaL) system. The DiGiTaL algorithms use dual-frequency GPS pseudorange and carrier-phase observables provided by the onboard GNSS receiver to compute state estimates with <1 cm relative position accuracy and 1m absolute position accuracy [7]. DiGiTaL requires crosslink communication between the spacecraft to exchange measurements and similar spacecraft attitudes to maximize the number of commonly visible GNSS satellites.

Maneuver planning is accomplished using closed-form solutions with flight heritage on PRISMA [8] and TanDEM-X [9] when maximum accuracy is not required. When performing science observations, a stochastic model predictive controller (SMPC) is employed to simultaneously maximize control accuracy and minimize computation effort. The SMPC also minimizes propellant expenditure by using a new fuel-optimal impulsive maneuver planning algorithm [10]. This algorithm produces maneuver plans consisting of 3-6 impulses with a total ΔV cost within a user-specified tolerance of a rigorous lower bound. More details on the SMPC are provided in [11].

Throughout the mission, only one spacecraft, denoted as the deputy, will be actively maneuvering with respect to the second spacecraft, denoted as the chief. This chief-deputy architecture is a common design solution for satellites

conducting proximity operations and lowers the on-orbit complexity by restricting maneuver planning and execution to be conducted by a single spacecraft. The OSC and DSC will host identical GNC software, thus allowing the chief and deputy roles to be interchangeable between spacecraft. This capability entails that the total available ΔV is the sum of the ΔV provided by each spacecraft and offers a level of robustness in the event of an anomaly on either spacecraft that prevents maneuverability, which is critical for the safety plan discussed in Section IV. Role switching will occur either autonomously in the event of an anomaly via the ISL or by an uplinked command from a ground station.

C. Inter-Satellite Crosslink

As mentioned, the relative navigation algorithm imparts a requirement for constant communication regardless of orientation; this ISL is achieved with the Inter-Satellite Crosslink (XLINK) system designed by the VISORS mission team. The crosslink system provides near full sky coverage with a communication range of 2 meters to 10 kilometers. The system works by having a patch antenna on each side of the spacecraft. The antennae use a set of four ADRV9009 radios two of which live on the FPGA board while the other two are found on the accompanying daughter board. Diplexers are used between the antennae and radios to combine the receive and transmit lines into one line leading to each antenna. A gain amplifier is also used when transmitting to an antenna to increase the bandwidth. The system transmits and receives using 5.8 GHz frequency band. The FPGA in this system is responsible for the controller that activates one radio and one antenna at a time. It is also responsible for discovering which antennae can maintain the link as the spacecraft's attitudes change over time, link establishment, and link maintenance. The XLINK system layout is shown in Fig 7.

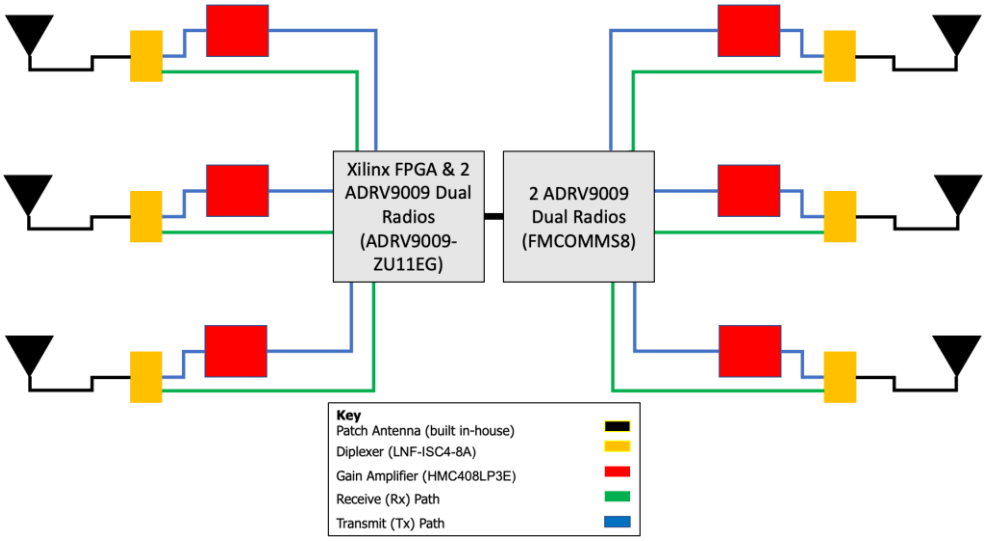

Fig. 7 Inter-satellite Crosslink (XLINK) system block diagram

D. Propulsion

As discussed, a 3DOF propulsion system is a key technology requirement which enhances the likelihood of mission success. The VISORS mission utilizes a 3D printed cold gas thruster propulsion system developed by team member Georgia Tech. The system currently has a TRL-6 as it leverages from previous systems designed for the BioSentinel, INSPIRE, and Ascent CubeSat missions [12]. Shown in Fig. 5 and Fig. 6, the propulsion system is located at the bottom of the VISORS spacecrafts. In Fig. 8, the main dimensions and locations of components are shown.

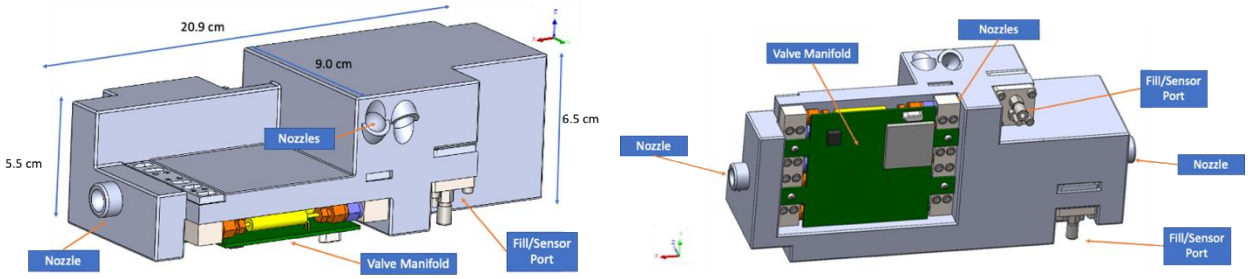

Fig. 8 Propulsion system CAD model and component layout.

The propulsion system uses R-236fa commercially available refrigerant, and the 3D printed structure is comprised of Somos PerFORM material. The system contains two tanks: the main tank and the plenum. The propellant is stored as a saturated mixture and at the saturation pressure in the main tank, and the propellant in the plenum is in a vapor state. When a propulsive maneuver is to be executed, the required thruster valves open and allow the vaporized propellant to exit from the corresponding nozzles. The plenum must be refilled when its pressure drops below 80% of the main tank pressure to ensure a minimum efficiency and obtains an influx of propellent from the main tank via a refill valve. Each tank also has a pressure and temperature sensor which is used to determine when to refill the plenum, to determine the duration of propulsive maneuvers, and to monitor the health of the system. A block diagram representation of the system is shown in Fig. 9. The thruster valves as well as the pressure and temperature sensors for the tanks are controlled by a radiation-tolerant ATmegaS128 microcontroller.

The system contains six nozzles as denoted in Fig. 9. Two nozzles are aligned with the body X-axis of the spacecraft as shown in Fig. 5 and Fig. 6. Due to the surface area availability of the propulsion system on each spacecraft, a nozzle cannot be pointed solely in the body -Z direction. To retain the decoupling between attitude maneuvers and thrust maneuvers, the remaining four nozzles are canted by 45° to exist in the YZ plane. When propellant exits a canted nozzle, a thrust component occurs along a ±Y and a ±Z direction. This results in a set of 6 nozzles whose pointing vectors are either anti-parallel or orthogonal to one another. Two of these canted nozzles are depicted in Fig. 8, and the cant directions are explicitly stated in the nozzle nomenclature in Fig. 9.

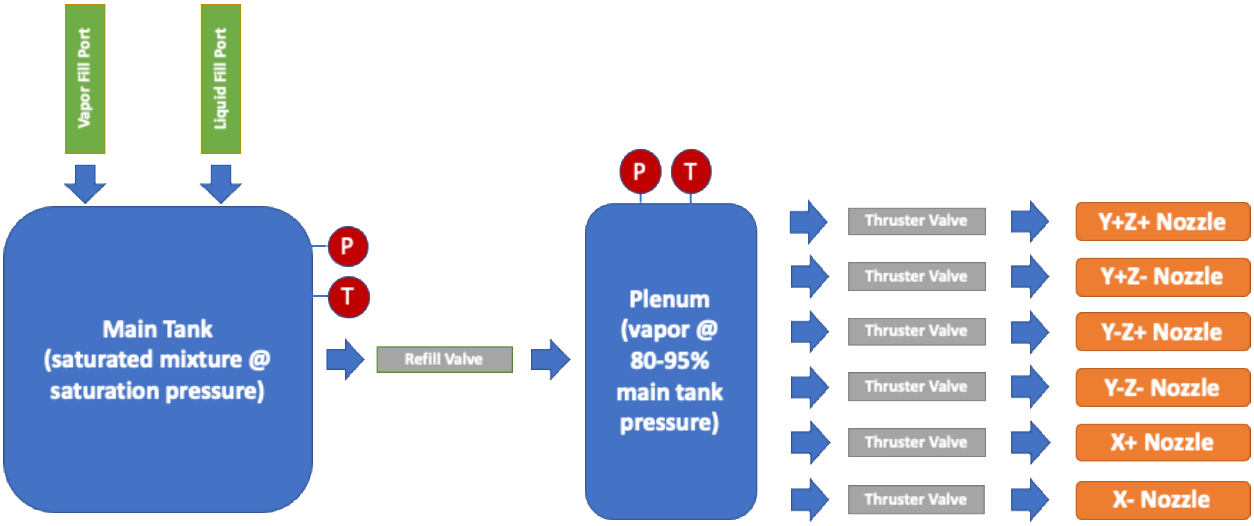

Fig. 9 Fluid block diagram of propulsion system with the nomenclature of the nozzle referring to its pointing direction.

Due to prior performance characterization activities of heritage systems, the performance of the VISORS system is well established [12]. The system can produce a minimum impulse bit of 200 μN∗s and contains 0.28 kg of propellant in the 237 cm^3 main tank as shown in Table 2. Based on the propellant capacity and a nominal 12 kg weight of the spacecraft, each spacecraft has a ΔV budget of 8 m/s. With two spacecrafts, there is a total ΔV of 16 m/s in the mission.

Table 2. Propulsion system performance parameters.

Parameter	Value	Parameter	Value
Wet Mass (kg)	1.32	Main Tank Volume (cm^3)	237
Dry Mass (kg)	1.04	Delta V per Spacecraft (m/s)	8.0
Propellant Mass (kg)	0.28	Time to Deplete Plenum (s)	1.7 @ -5°C 1.5 @ 50°C
Plenum Volume (cm^3)	69.3	Time to Refill Plenum (s)	~3 across operating range
Minimum Impulse Bit (μN*s)	200 (nominally)	Valve Timing Resolution (ms)	1

The current mission timeline assumes 10 relative orbit transitions between the standby and science relative orbits, 10 orbits in the science relative orbit prior to reverting to the standby orbit, 1 collision avoidance maneuver with a subsequent reacquisition of standby mode, and a total mission timeline of 90 days. Using this timeline, the ΔV budget for the mission with the cost breakdown of each propulsive maneuver shown in Table 3 was constructed. Currently, there is approximately 3 m/s of unallocated ΔV in the budget. If additional collision avoidance maneuvers are required during operations, this unallocated ΔV can be utilized without sacrificing the ΔV required for the notional mission timeline. Leftover ΔV after completion of the notional mission will be used for additional relative orbit transfers and thus more science observation attempts.

Table 3. Mission ΔV budget with cost and number of occurrences for each propulsive maneuver type.

Maneuver Type	ΔV (m/s)	# of Occurances	Discrete # of Occurances	Total ΔV (m/s)	Contingency (%)	Max Expected ΔV (m/s)
Orbit Formation	1	1	1	1	50	1.5
Rel. Orbit Stationkeeping	0.11	12.857	13	1.43	10	1.573
Science Mode Entry	0.3	10.0	10	3	10	3.300
Science Mode Maintenance	0.026	100.0	100	2.6	10	2.860
Science Mode Exit	0.3	10.0	10	3	10	3.300
Collision Avoidance	0.15	1.0	1	0.15	10	0.165
Standby Mode Reacquistion	0.3	1.0	1	0.3	10	0.330
Total				**11.180**	**14.18%**	**13.028**
Allowances			**Unallocated ΔV (m/s)**		**2.972**	**16**

E. Payload Avionics Board

The avionics board performs several functions that ensure the different payload subsystems work together and with the spacecraft bus. First, it manages data interfaces between the BCT bus and the different payload subsystems: propulsion, XLINK, and detector instrument. The board also provides nonvolatile storage for science observation data and telemetry data for downlinking. Finally, the board is also responsible for distributing and monitoring power from the bus to the payload subsystems. Fig. 5 and Fig. 6 show the component placed in the spacecraft while Fig. 10 shows the preliminary board layout for the spacecrafts.

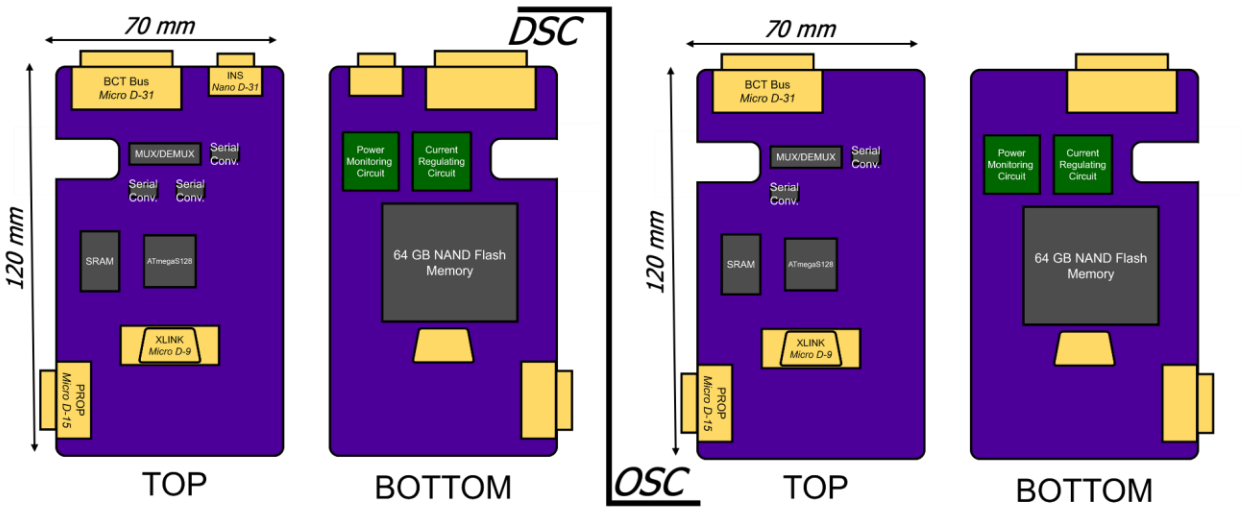

Fig. 10 DSC and OSC avionics board layout.

The board utilizes the radiation-tolerant ATmegaS128 microcontroller to perform its functions, which have flight heritage with the Lunar Flashlight and GT-1 CubeSat missions [13]. The processor provides 2 UART, 1 SPI, and 1 I2C serial interface lines. As shown in Fig. 11, a single UART line is used to interface with the BCT bus while the other UART line is used to interface between the three payload subsystems. Because the payload subsystems share a single UART line, a multiplexer with interruption capabilities and channel priorities must be used to regulate traffic on the line. The SPI lane is dedicated to reading and writing to the nonvolatile 64 GB flash storage. Finally, the I2C line is allocated for current and voltage monitoring for all outputs. Power is delivered from the BCT bus but is regulated and distributed by the avionics board. Via buck converters, the board can provide regulated 3.3, 5, 9, and unregulated 12 V power supply to the different subsystems. The DSC and OSC share near-identical designs for their avionics boards; the main exception is that the DSC avionics board contains an interface and power monitoring capability for the detector instrument.

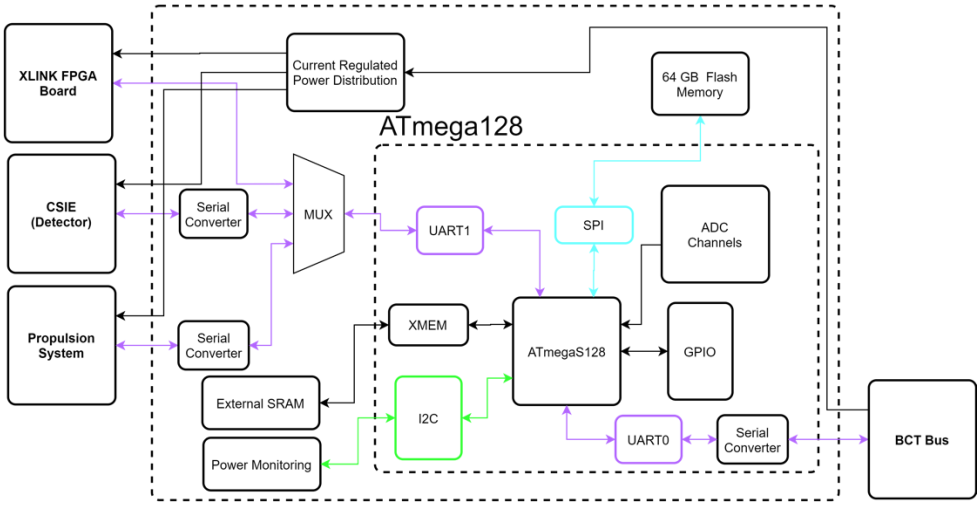

Fig. 11 Avionics board interface diagram for the DSC. OSC is similar but does not include the *CSIE (detector)* block and its respective inputs.

IV. Mission Safety Plan

A. Contingency Plans

As mentioned in Section II.B, a mission safety plan was developed by analyzing the concept of operations with the current spacecraft design to arrive at a set of contingency plans that the formation will be programmed to autonomously complete depending on the key parameters mentioned in the above subsection. The passive safety due to E/I vector separation serves as the first deterrent for a collision and thus any active collision avoidance plan will only be executed if any or all spacecraft experience an anomaly for a duration of time which compromises this passive safety. The set of possible anomalies can be divided into two groups: an error recognized by the bus results in a shutdown of payload systems and a transition into a bus safe mode, and an outage or failure of a subsystem. The errors recognized by the bus can be further divided: errors which arise when measurable quantities exceed their bounds, such as reaction wheels reaching their peak spin rates, and single-event errors that occur at random. The measurable quantities can be monitored by their respective spacecraft, and for single-event errors the bus will be able to transmit a message on the ISL; both these features are critical in the safety plan procedures.

If any anomaly occurs when the formation is in science mode, the deputy role is assigned to the functional spacecraft via an ISL transmission. Then the new deputy spacecraft waits a predetermined, specified time for the inhibited chief spacecraft to regain its nominal functionality. If so, the chief spacecraft will establish an ISL with the deputy spacecraft and nominal science mode operations will resume. If the chief spacecraft cannot regain nominal functionality before the specified time, the deputy spacecraft will complete a maneuver sequence which transfers the formation in standby mode. The deputy can complete this maneuver sequence without measurements from the chief spacecraft and reverting to standby mode allows for greater passive safety margin as the operations team begins troubleshooting. The contingency plan is almost identical if an anomaly occurs as the formation is transferring into or out of the science formation, with the sole difference being that the predetermined waiting time is longer than for the science mode contingency plan since the spacecraft are farther apart. If the formation is in standby mode at the time of an anomaly, then the new deputy role will still be established, and the formation remains in this mode during troubleshooting. This set of contingency plans is less nuclear as it retains autonomous formation-keeping and allows for a rapid turnaround to nominal operations once both spacecraft have regained nominal functionality.

The second set of contingency plans revolves around the use of a collision avoidance maneuver. This maneuver increases the inter-satellite range along the radial and cross-track directions while introducing a drift in the along-track direction, which guarantees continual passive safety but requires an uplinked maneuver plan re-establish the standby relative orbit. Any inhibited spacecraft will be troubleshooted from the ground and upon successful return to nominal spacecraft operations, an uplinked maneuver plan will be transmitted to the deputy spacecraft to re-establish the relative orbit in standby mode. If either spacecraft detect a potential collision within the next two orbits, then the collision avoidance maneuver will be planned and executed at least one orbit prior to the expected collision event. If one spacecraft is already in a safe mode due to an anomaly and the new deputy spacecraft has received a safe mode command from the bus, then the deputy spacecraft will execute the collision avoidance maneuver prior to entering its safe mode. Since the time at which either spacecraft exits its respective safe mode is unknown, executing the collision avoidance maneuver provides ample time for troubleshooting without realizing the risk of collision.

B. Risk Analysis

In the mission, the formation can experience myriad different combinations of anomalies with widely varied severity and unknown down times before restoration of nominal functionality. These combinations are grouped into cases, and the contingency plans mentioned in the prior section are evaluated against these cases to determine which risks are reducible (i.e. mitigated by the contingency plan) and which are irreducible. The reducible risk cases are shown in Fig. 12. Note that for each case, any subset of highlighted subsystems also falls under that case. For example, Case 1 has permanent failures of the propulsion and GNC subsystems of the OSC. If only the propulsion system exhibits a permanent failure, this scenario is also captured by Case 1. Cases 1 and 2 represent permanent loss of control on a single spacecraft. Cases 3 through 5 represent safe mode occurrences on any or all spacecraft. Case 6 highlights scenarios with temporary outages in the ISL, GNSS receiver, and attitude control system. Cases 7 and 8 are scenarios where anomalies are encountered potentially across all subsystems on a single spacecraft, but the ISL remains operational. These 8 cases and their subsets are all off-nominal scenarios the formation may experience in the mission and are mitigated by the safety plan.

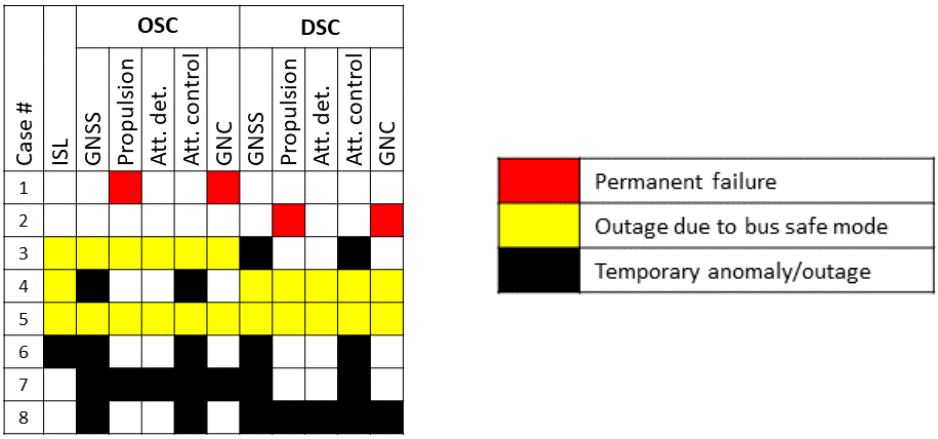

Fig. 12 Chart of reducible risk cases.

However, cases do exist where multiple combined outages or permanent failures significantly increases the risk of collision or result in the end of mission due to the inability to meet the mission objectives, respectively. These cases carry an irreducible risk that is not mitigated by the contingency plan. The irreducible risk cases are shown in Fig. 13. Similar to the reducible risk cases, any subset of highlighted subsystems in any irreducible risk case (but does not fall into one of the cases in Fig. 12) also falls under that case. Case 9 occurs for single component failures in the ISL, GNSS receiver, or the ADCS system on either or both spacecraft. Case 10 represents a total loss of translational maneuverability. Both cases 9 and 10 result in an end of mission as permanent losses of these critical subsystems or degradation of performance beyond acceptable levels results in the inability to meet mission objectives. Case 11 represents temporary anomalies in the deputy spacecraft and the ISL, thus preventing a chief-deputy role switch to occur. Case 12 reflects simultaneous anomalies that inhibit maneuver planning and execution on both spacecraft. Although Cases 11 and 12 only involve temporary outages, the inability of the formation to maneuver poses an increased collision risk since the time to return to nominal functionality may be greater than the passive safety margin provided by the relative orbit.

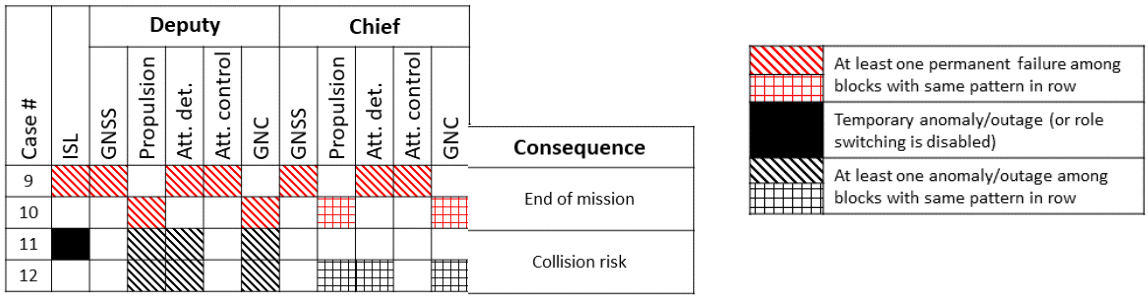

Fig. 13 Chart of irreducible risk cases.

Fig. 14 depicts a Likelihood-Consequence (LC) chart for the aforementioned 12 cases. The contingency plan does reduce the risk of collision in a wide variety of scenarios, and this is reflected in the LC chart by the fact that all cases between 1 and 8, which are the reducible risk cases, have a "Consequence" value of 3 or lower. Case 9 highlights the single point-of-failure subsystems and how they pose a significant end-of-mission risk. Furthermore, Cases 11 and 12 demonstrate how certain subsets of temporarily disabled subsystems can impose a significant collision risk if they are not brought back to nominal functionality within the passive safety margin. The VISORS mission team intends to track and investigate the findings from Cases 9, 11, and 12 as the mission progresses and if possible, either update the spacecraft design or augment the safety plan to lower the probability of occurrence or even transform them into reducible risk cases.

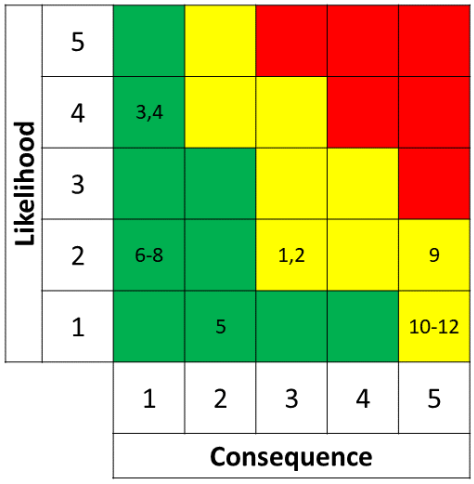

Fig. 14 Likelihood-Consequence chart for potential off-nominal scenarios.

V. Upcoming Milestones

This paper summarizes the preliminary design of the VISORS formation, and this solution will undergo several internal design and flight readiness reviews prior to launch to ensure that the system meets its requirements. The preliminary design review occurred in the 4th quarter of 2020 and will be followed by the critical design review in the 3rd quarter of 2021. A pre-ship review will be conducted in the 4th quarter of 2022 to serve as the final checkpoint before spacecraft shipment to the launch provider. A mission readiness review will occur in the 2nd quarter of 2023 which leads into the extended launch time frame of the 3rd quarter in 2023.

VI. Conclusion

The image resolution necessary to observe the existence of thin, heat-release regions in the solar corona is unachievable by scaling current technologies in diffractive optics. This paper presents an alternate approach that utilizes a CubeSat formation to create a distributed space telescope, but stringent relative state requirements are derived from the science goals. The VISORS team is unaware of a flown, CubeSat formation-flying mission that has maintained relative states on this scale, and innovative technologies in relative orbit GNC, communications and propulsion were sought in the proposal stage to accomplish this objective. The development of a feasible concept of operations, design and integration of each subsystem into a two 6U spacecraft formation while assessing collision risks to gauge mission safety all serve as challenging engineering problems that this paper addresses at a preliminary design level. The preliminary design review completed in Q4 2020 served as a major checkpoint to evaluate this system design and assess the path forward for a critical design review, system integration and test, which will be conducted by the VISORS mission team upon delivery of the 6U buses, and a late 2023 launch.

Acknowledgments

This material is based upon work supported by the National Science Foundation under Contract No. 1936576. Any opinions, findings, and conclusions or recommendations expressed in this material are those of the author(s) and do not necessarily reflect the views of the National Science Foundation.

The authors recognize the VISORS team, listed in Table 4, for their continued support throughout the mission. The content in this paper was derived from internal documents that were created and managed by the team but are currently not subjected to external review. Furthermore, the authors recognize the efforts of the bus vendors for their cooperation as a 6U bus design is finalized.

Table 4: VISORS mission team.

Participant	Institution
Farzad Kamalabadi (PI), Endowed Professor	**Univ. of Illinois**, Electrical and Computer Eng.
Alina Alexeenko, Professor	**Purdue Univ.**, Aeronautics & Astronautics
Philip Chamberlin, Research Scientist	**Univ. of Colorado**, LASP
Simone D'Amico, Assistant Professor	**Stanford Univ.**, Aeronautics & Astronautics
Adrian Daw, Research Astrophysicist	**NASA GSFC**, Heliophysics Science Division
Kevin Denis, Electrical Engineer	**NASA GSFC**, Instrument Systems and Tech. Division
Eylem Ekici, Professor	**Ohio State Univ.**, Electrical & Computer Eng.
Subhanshu Gupta, Assistant Professor	**Washington State Univ.**, Electrical Eng.
John Hwang, Assistant Professor	**Univ. of Calif. San Diego**, Mechanical & Aerosp. Eng.
James Klimchuk, Research Astrophysicist	**NASA GSFC**, Heliophysics Science Division
Glenn Lightsey, Professor	**Georgia Tech**, Aerospace Eng.
Hyeongjun Park, Assistant Professor	**New Mexico State Univ.**, Mechanical & Aerosp. Eng.
Douglas Rabin, Research Astrophysicist	**NASA GSFC**, Heliophysics Science Division
John Sample, Assistant Professor	**Montana State Univ.**, Physics
Thomas Woods, Associate Director	**Univ. of Colorado**, LASP

References

[1] Peter, H. and Dwivedi, B., "Discovery of the Sun's Million-degree Hot Corona," Frontiers in Astronomy and Space Sciences, Vol. 1, no. 2, 2014. doi:10.3389/fspas.2014.00002

[2] Geospace Section, Division of Atmospheric and Geospace Sciences, [National Science Foundation], "Geospace Sciences: The Study of the Space Environment of Planet Earth," April 2013. https://cedarweb.vsp.ucar.edu/wiki/images/9/9f/NSF_GS_Plan_June_2013.pdf [retrieved 30 March 2020]

[3] Attwood, D., Soft X-Rays and Extreme Ultraviolet Radiation: Principles and Applications, Cambridge, UK: Cambridge University Press, 1999.

[4] D'Amico S., Montenbruck O., "Proximity Operations of Formation-Flying Spacecraft Using an Eccentricity/Inclination Vector Separation." Journal of Guidance, Control, and Dynamics. Vol 29, No. 3, May-June 2006. doi: 10.2514/1.15114

[5] Reising, S., Gaier, T.C., Kummerow, C., Padmanabhan, S., Lim, B.H., Heneghan, C., Chandrasekar, V., Berg, W., Olson, P., Brwon, S.T., Carvo, J., Pallas, M. "Temporal Experiment for Storms and Tropical Systems Technology Demonstration (TEMPEST-D) Mission: Enabling Time-Resolved Cloud and Precipitation Observations from 6U-Class Satellite Constellations," *Proceedings of the AIAA/USU on Small Satellites,* Next on the Pad, SSC17-III-01. https://digitalcommons.usu.edu/smallsat/2017/all2017/78/ [retrieved 20 November 2020]

[6] Smith, M., Donner, A. Knapp, M., Pong, C., Smith, C., Luu, J., Pasquale, P., Campuzano, B. 2018. "On-Orbit Results and Lessons Learned from the ASTERIA Space Telescope Mission," *Proceedings of the AIAA/USU on Small Satellites*, The Year in Review, SSC18-1-08. https://digitalcommons.usu.edu/cgi/viewcontent.cgi?article=4067&context=smallsat [retrieved 28 September 2020].

[7] D'Amico S., Hunter R., Baker C., "Distributed Timing and Localization (DiGiTaL)" NASA Technical Reports Server 2017 https://ntrs.nasa.gov/search.jsp?R=20170011077

[8] D'Amico, S., "Autonomous Formation Flying in Low Earth Orbit," PhD Thesis, Delft University, 2010.

[9] Ardaens, J.-S., and Fischer, D., "TanDEM-X Autonomous Formation Flying System: Flight Results," IFAC Proceedings, Vol. 44, No. 1, 2011, pp. 709–714.

[10] Koenig, A. W. and D'Amico, S., "Fast Algorithm for Fuel-Optimal Impulsive Control of Linear Systems with Time-Varying Cost," IEEE Transactions on Automatic Control, 2020.

[11] Koenig, A. W., D'Amico, S., and Lightsey, E. G., "Formation Flying Orbit and Control Concept for the VISORS Mission," AIAA SciTech 2021 Forum, Nashville, TN, 2021.

[12] Lightsey, E.G., Stevenson, T., and Sorgenfrei, M., "Development and Testing of a 3-D-Printed Cold Gas Thruster for an Interplanetary CubeSat." Proceedings of the IEEE, Vol. 106, No. 3, pp. 379-390, March 2018. doi: 10.1109/JPROC.2018.2799898

[13] Wilk, M.; Lightsey, E.G., "Development of Maneuverable Deep Space Small Satellites," retrieved November 2020. https://ssdl.gatech.edu/sites/default/files/ssdl-files/papers/mastersProjects/WilkM-8900.pdf